

A New Numerical Method for \mathbb{Z}_2 Topological Insulators with Strong Disorder

Yutaka Akagi^{1*}, Hosho Katsura¹, and Tohru Koma²

¹*Department of Physics, Graduate School of Science, The University of Tokyo, Hongo, Tokyo 113-0033, Japan*

²*Department of Physics, Gakushuin University, Mejiro, Toshima-ku, Tokyo 171-8588, Japan*

We propose a new method to numerically compute the \mathbb{Z}_2 indices for disordered topological insulators in Kitaev's periodic table. All of the \mathbb{Z}_2 indices are known to be derived from the index formulae which are expressed in terms of a pair of projections introduced by Avron, Seiler, and Simon. For a given pair of projections, the corresponding index is determined by the spectrum of the difference between the two projections. This difference exhibits remarkable and useful properties, as it is compact and has a supersymmetric structure in the spectrum. These properties make it possible to numerically determine the indices of disordered topological insulators highly efficiently. The method is demonstrated for the Bernevig-Hughes-Zhang and Wilson-Dirac models whose topological phases are characterized by a \mathbb{Z}_2 index in two and three dimensions, respectively.

KEYWORDS: Topological insulators, Time reversal symmetry, \mathbb{Z}_2 topological invariant, disordered systems

Since the discovery of \mathbb{Z}_2 topological insulators by Kane and Mele,¹⁾ many methods have been proposed to compute the \mathbb{Z}_2 index. In particular, Fu and Kane found that the calculation of the \mathbb{Z}_2 index can be considerably simplified in a system with inversion symmetry.²⁾ However, for disordered systems, a numerical determination of the \mathbb{Z}_2 index is still very challenging. Roughly speaking, three types of numerical methods have been proposed so far for this problem:

- The first one was proposed by Kane and Mele themselves,¹⁾ and later some modifications were introduced. Basically, for a given model, the \mathbb{Z}_2 index is defined by a certain Pfaffian with twisted boundary conditions.³⁾ The methods were applied to class AII models⁴⁻⁶⁾ in two and three dimensions with or without a certain inversion symmetry.⁷⁻⁹⁾
- The second one is based on a scattering matrix theory.¹⁰⁾ The \mathbb{Z}_2 indices which are defined by the scattering matrices were numerically computed for models in the classes, AII and DIII, in two and three dimensions.^{10,11)}
- The third one was proposed by Loring and Hastings.¹²⁾ The \mathbb{Z}_2 indices are defined by Bott indices which are introduced as an obstruction to approximating almost commuting matrices. For models in the class AII in two and three dimensions, the \mathbb{Z}_2 indices were numerically computed.^{12,13)} For systems with chiral symmetry, Loring and Schulz-Baldes¹⁴⁾ proposed a numerical method to obtain the values of Bott indices.

In this paper, we propose an alternative method to numerically calculate the \mathbb{Z}_2 indices for disordered topological insulators in arbitrary dimensions. The method is based on the index formulae which were derived in Refs. [15, 16], and has the following two advantages: (i) There is no need to take an average of the \mathbb{Z}_2 index over random variables in a model. (ii) The \mathbb{Z}_2 index is determined by the discrete spectrum of a certain compact operator with a supersymmetric structure. The latter makes it possible to numerically determine the \mathbb{Z}_2 index

highly efficiently.

Our method is demonstrated for Bernevig-Hughes-Zhang (BHZ)¹⁷⁻¹⁹⁾ and Wilson-Dirac²⁰⁻²²⁾ models whose topological phases are characterized by a \mathbb{Z}_2 index of the class AII in two and three dimensions, respectively. In consequence, the method enables us to determine all of the values of the \mathbb{Z}_2 indices of the strong and weak topological insulators, and the normal insulator phases in the phase diagrams. These values of the \mathbb{Z}_2 indices completely coincide with the predictions in previous studies using a reliable transfer-matrix method.^{18,19,22)}

To begin with, we introduce two Dirac operators as^{15,16)}

$$\mathcal{D}_{\mathbf{a}}(\mathbf{x}) := \frac{x_1 + ix_2 - (a_1 + ia_2)}{|x_1 + ix_2 - (a_1 + ia_2)|} \quad (1)$$

in two dimension (2D), and

$$D_{\mathbf{a}}(\mathbf{x}) := \frac{1}{|\mathbf{x} - \mathbf{a}|}(\mathbf{x} - \mathbf{a}) \cdot \boldsymbol{\sigma} \quad (2)$$

in three dimensions (3D), where $\mathbf{x} = (x_1, \dots, x_d) \in \mathbb{Z}^d$ is the position operator and $\mathbf{a} = (a_1, \dots, a_d) \in \mathbb{R}^d \setminus \mathbb{Z}^d$ is a vector for $d = 2, 3$ [see Fig. 1(a)]. The three-component vector $\boldsymbol{\sigma}$ is defined by $\boldsymbol{\sigma} = (\sigma_1, \sigma_2, \sigma_3)$ whose components are given by Pauli matrices σ_i , each of which acts on an auxiliary Hilbert space \mathbb{C}^2 . The whole Hilbert space is given by the tensor product of the auxiliary \mathbb{C}^2 and the original Hilbert space for the Hamiltonian of tight-binding models which we will consider shortly.

Next, we define the \mathbb{Z}_2 index for an infinite-volume system which is a tight-binding model on a square \mathbb{Z}^2 or cubic lattice \mathbb{Z}^3 .²³⁾ Let P_F be the projection operator onto the states below the Fermi energy E_F . The difference of two projections is defined as^{16,24)}

$$A := \begin{cases} P_F - \mathcal{D}_{\mathbf{a}}^* P_F \mathcal{D}_{\mathbf{a}} & \text{in 2D} \\ P_F - D_{\mathbf{a}} P_F D_{\mathbf{a}} & \text{in 3D,} \end{cases} \quad (3)$$

where $\mathcal{D}_{\mathbf{a}}^*$ is the adjoint of the Dirac operator $\mathcal{D}_{\mathbf{a}}$. Then,

*E-mail address: akagi@cams.phys.s.u-tokyo.ac.jp

the \mathbb{Z}_2 index ν is defined as

$$\nu = \dim \ker (A - 1) \text{ modulo } 2. \quad (4)$$

When the Fermi energy E_F lies in a spectral gap or a mobility gap, the \mathbb{Z}_2 index is known to be well defined.¹⁶⁾ In the following, we will consider such situations.

Now we describe our numerical scheme for calculating the \mathbb{Z}_2 index. Let Λ and Ω be two finite regions satisfying $\Omega \subset \Lambda \subset \mathbb{R}^d$ and $\mathbf{a} \in \Omega$ as in Fig. 1. First, we approximate the Fermi projection P_F in the infinite volume by the corresponding Fermi projection in the finite region Λ . More precisely, the approximate one is given by

$$P_F^{(\Lambda)} := \sum_{E_n \leq E_F} |n\rangle \langle n|, \quad (5)$$

where $|n\rangle$ are eigenstates of the tight-binding Hamiltonian \mathcal{H} on Λ which we consider, and we have denoted by E_n the corresponding eigenvalues. To avoid the presence of gapless edge/surface states, we impose periodic boundary conditions for the Hamiltonian in practical numerical calculations. For the operator A in Eq. (3), we replace the Fermi projection P_F by $P_F^{(\Lambda)}$, and write $A^{(\Lambda)}$ for the approximate one. Further, we restrict the operator $A^{(\Lambda)}$ to the subregion Ω as

$$A_\Omega^{(\Lambda)} := \chi_\Omega A^{(\Lambda)} \chi_\Omega, \quad (6)$$

where χ_Ω is the characteristic function of the subregion Ω .

Under the above gap assumption, the operator A in Eq. (3) is compact even in the infinite volume limit. Therefore, the spectrum of A is discrete and has no accumulation point except for zero. This implies that an eigenstate of A is localized if the corresponding eigenvalue is not equal to zero. Let $\lambda \neq 0$ be an eigenvalue of A . From these observations, it is clear that the eigenvalue λ can be approximated by an eigenvalue λ' of the approximate operator $A_\Omega^{(\Lambda)}$ if the subregion Ω is sufficiently large. In addition to this, the cutoff function χ_Ω in Eq. (6) enables us to remove the boundary effects due to the finite size of the region Λ .

As the first demonstration, we compute the \mathbb{Z}_2 index of the BHZ model¹⁷⁻¹⁹⁾ with disorder on a square lattice \mathbb{Z}^2 . The Hamiltonian is written as

$$\mathcal{H}_{2D} = \sum_{\mathbf{x}} \sum_{k=1,2} [c_{\mathbf{x}}^\dagger t_k c_{\mathbf{x}+\mathbf{e}_k} + \text{h.c.}] + \sum_{\mathbf{x}} c_{\mathbf{x}}^\dagger (\tau_0 \otimes \epsilon_{\mathbf{x}}) c_{\mathbf{x}}, \quad (7)$$

where $c_{\mathbf{x}} = [c_{\mathbf{x}1\uparrow}, c_{\mathbf{x}1\downarrow}, c_{\mathbf{x}2\uparrow}, c_{\mathbf{x}2\downarrow}]^T$, and $c_{\mathbf{x}i\alpha}$ is the annihilation operator of an electron with spin α and orbital i at site \mathbf{x} . The hopping matrices, t_1 and t_2 , are given by $t_1 = g_1 \tau_0 \otimes s_3 - \frac{i}{2} g_2 \tau_0 \otimes s_2 + \frac{i}{2} g_3 \tau_2 \otimes s_3$, and $t_2 = g_1 \tau_0 \otimes s_3 - \frac{i}{2} g_2 \tau_3 \otimes s_1 - \frac{i}{2} g_3 \tau_2 \otimes s_0$, where τ_k and s_k ($k = 1, 2, 3$) are Pauli matrices for the orbital and the spin, respectively. Here, g_1, g_2 and g_3 are real parameters. The on-site potential $\epsilon_{\mathbf{x}}$ is given by $\epsilon_{\mathbf{x}} = \text{diag}[\Delta - 4g_1 + W_{\mathbf{x}}^+, -\Delta + 4g_1 + W_{\mathbf{x}}^-]$, where $W_{\mathbf{x}}^+$ and $W_{\mathbf{x}}^-$ are a random potential whose distribution is uniform in the interval $[-W/2, W/2]$ with a positive parameter W . \mathbf{e}_1 and \mathbf{e}_2 are the unit vectors in the x and y directions, respectively. As is well known,¹⁷⁻¹⁹⁾ this

Hamiltonian (7) belongs to the symmetry class AII. We set the Fermi energy $E_F = 0$ which is located at the center of the energy gap.

In the following, we write λ_i for the i -th eigenvalue of the operator $A_\Omega^{(\Lambda)}$ of Eq. (6) in descending order including multiplicity.²⁵⁾ We note that the spectrum of $A_\Omega^{(\Lambda)}$ is included in the interval $[-1, 1]$.

Before showing our numerical results, we abbreviate the topological and the ordinary insulator phases as TI and OI, respectively, in the phase diagram,^{18,19)} and write ν for the value of the \mathbb{Z}_2 index. Figure 1(c) and (d) show, respectively, λ_1 and $\lambda_1 - \lambda_2$ as a function of the mass Δ and the strength W of disorder. In the region TI, our numerical results are satisfactory because $\lambda_1 \simeq 1$ and $\lambda_1 - \lambda_2 \neq 0$. Actually, these imply $\nu = 1$, i.e., the phase is topological as we expected. In the region OI, λ_1 is significantly different from 1, and thus $\nu = 0$. These results show that the \mathbb{Z}_2 index enables us to distinguish TI from OI. In OI phase, one notices $\lambda_1 \simeq \lambda_2 \lesssim 0.2$ as seen in Fig. 1(d). This degeneracy is nothing but a consequence of the two symmetries,^{15,16)} the time-reversal symmetry of the Hamiltonian and the supersymmetric structure of the operator A . This kind of degeneracy is very useful to determine the \mathbb{Z}_2 index. In the region $W \lesssim 6$, our results are in good agreement with the previous results¹⁹⁾ which were obtained by using a transfer-matrix method. In the region with a sufficiently large W , Anderson localization is expected to occur. For the intermediate critical region between these two regions, our method is not under control because the existence of a significantly nonvanishing spectral or mobility gap cannot be expected. In fact, our numerical results in this region show large fluctuations in both λ_1 and $\lambda_1 - \lambda_2$.

The second example is the Wilson-Dirac model²²⁾ with disorder on the cubic lattice \mathbb{Z}^3 . The Hamiltonian is written as

$$\mathcal{H}_{3D} = \mathcal{H}_0 + \mathcal{H}_{\text{hop}} + \mathcal{H}_{\text{dis}}, \quad (8)$$

where

$$\begin{aligned} \mathcal{H}_0 &= \sum_{\mathbf{x}} \sum_{k=1,2,3} \left[\frac{it}{2} c_{\mathbf{x}+\mathbf{e}_k}^\dagger \alpha_k c_{\mathbf{x}} - \frac{m_2}{2} c_{\mathbf{x}+\mathbf{e}_k}^\dagger \beta c_{\mathbf{x}} + \text{h.c.} \right] \\ &+ (m + 3m_2) \sum_{\mathbf{x}} c_{\mathbf{x}}^\dagger \beta c_{\mathbf{x}}, \end{aligned} \quad (9)$$

$$\mathcal{H}_{\text{hop}} = \sum_{\mathbf{x}} \sum_{k=1,2,3} [t_0 c_{\mathbf{x}+\mathbf{e}_k}^\dagger c_{\mathbf{x}} + \text{h.c.}], \quad (10)$$

$$\mathcal{H}_{\text{dis}} = \sum_{\mathbf{x}} v_{\mathbf{x}} c_{\mathbf{x}}^\dagger c_{\mathbf{x}}. \quad (11)$$

Here, $c_{\mathbf{x}} = [c_{\mathbf{x}1\uparrow}, c_{\mathbf{x}1\downarrow}, c_{\mathbf{x}2\uparrow}, c_{\mathbf{x}2\downarrow}]^T$, the vector \mathbf{e}_k is the unit vector in $k = x, y, z$ direction, and $\alpha_k = \tau_1 \otimes s_k$, $\beta = \tau_3 \otimes s_0$; $v_{\mathbf{x}}$ is the on-site random potential whose distribution is uniform in the interval $[-W/2, W/2]$ with a positive parameter W . This Hamiltonian (8) belongs to the symmetry class AII for $W \neq 0$ or $t_0 \neq 0$. In the following, we will treat the case with $t_0 \neq 0$.

Similarly, we abbreviate the weak, strong topological, the ordinary insulator and the diffusive metal phases as WTI, STI, OI, and M, respectively,²²⁾ and write ν for

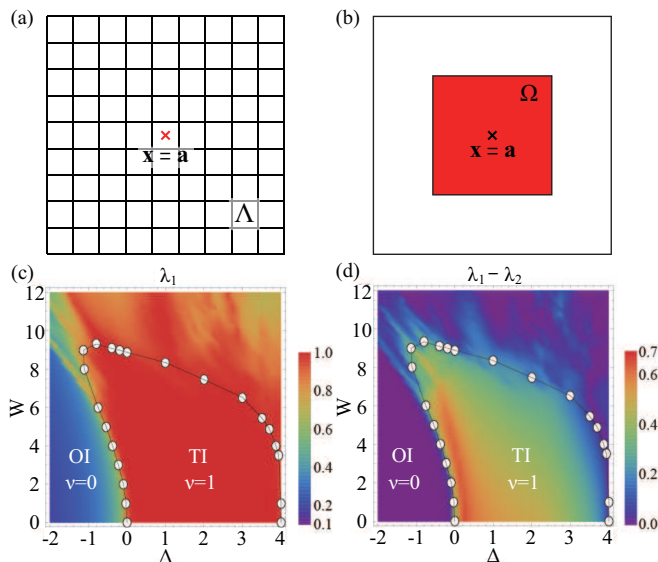


Fig. 1. (Color online). (a) The location of \mathbf{a} is chosen to be the center of the finite lattice Λ of linear size L . (b) The subregion Ω is chosen so that its center is the same as \mathbf{a} and it does not overlap with the boundary of Λ . (c) and (d), respectively, show λ_1 and $\lambda_1 - \lambda_2$ in the BHZ model as a function of the mass Δ and the disorder strength W . The obtained value ν of the \mathbb{Z}_2 index is indicated in both OI and TI phases. The values of the parameters used are $E_F = 0$, $g_1 = g_2 = 1$, $g_3 = 0$, and the system size is $L^2 = 1600$. The curves of the phase boundaries with the dots are plotted by using the results in Ref. [19].

the value of the \mathbb{Z}_2 index.²⁶⁾ Figure 2 shows λ_1 and $\lambda_1 - \lambda_2$ as a function of the mass parameter m_0/m_2 and the strength W/m_2 of disorder. In the region OI, $\nu = 0$ because $\lambda_1 \lesssim 0.8$. In the region STI, $\lambda_1 \simeq 1$ and $\lambda_1 - \lambda_2 \neq 0$, and hence $\nu = 1$. In the region WTI, $\lambda_1 = \lambda_2 \simeq 1$ but λ_3 is significantly different from 1 [see Fig. 3(b)], and hence $\nu = 0$ because the multiplicity of the eigenvalue $\lambda \simeq 1$ is two. As for the region M, we cannot expect our method to be effective because the spectral or mobility gap is expected to vanish if the metallic character of the spectrum is true. To summarize, as seen in Fig. 2, our numerical results for the \mathbb{Z}_2 index are in good agreement with the predictions of Ref. [22]. In particular, the phase boundaries between WTI and STI, and between STI and OI are considerably sharp. Moreover, although our method is expected to be useless in the metallic phase, there do not appear fluctuations like those in the two-dimensional case.

Although the \mathbb{Z}_2 index vanishes in both the OI and WTI phases, there is a definite difference between them as follows: OI phase yields no eigenvalue $\lambda \simeq 1$ while WTI phase yields the eigenvalue $\lambda \simeq 1$ which is doubly degenerate. If the eigenvalue $\lambda \simeq 1$ is related to surface states, one can expect, from our numerical results, that the multiplicity of $\lambda \simeq 1$ coincides with the number of Dirac cones which appear on the surface of the system. In fact, it was numerically observed in a generalized Kane-Mele model on a diamond lattice that WTI (STI) phase exhibits two surface Dirac cones (odd number of Dirac cones).²⁷⁾

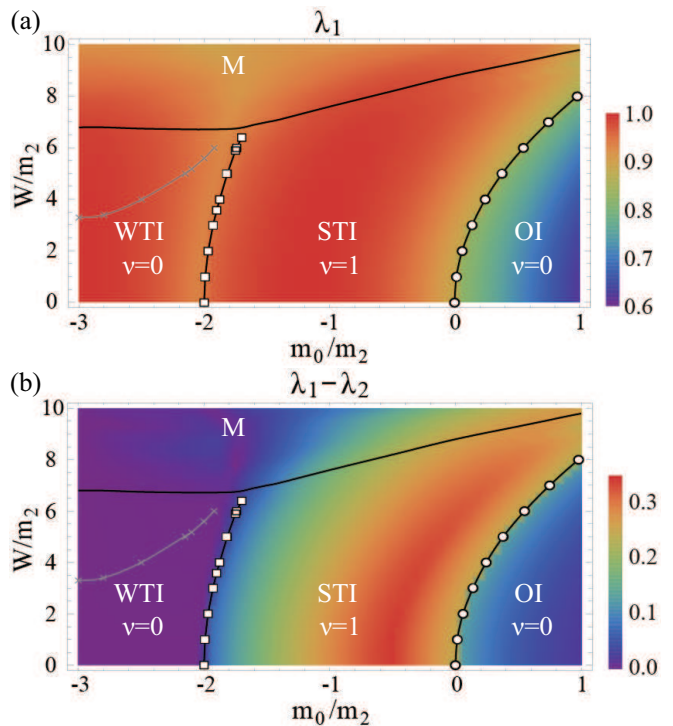


Fig. 2. (Color online). (a) and (b), respectively, show λ_1 and $\lambda_1 - \lambda_2$ in the Wilson-Dirac-type model as a function of the mass parameter m_0/m_2 and the disorder strength W/m_2 . The numerical values ν of the \mathbb{Z}_2 index are indicated in the phases WTI, STI and OI. The parameters used are $E_F = 0$, $t = 2$, $t_0 = 0.01$, and the system size is $L^3 = 1728$. The curves of the phase boundaries with the dots are plotted by using the results in Ref. [22].

Figure 3 shows W/m_2 and m_0/m_2 dependences of the eigenvalues λ_i , $i = 1, 2, \dots, 5$, of the operator $A_\Omega^{(\Lambda)}$. According to Ref. [22], STI emerges for $W/m_2 \lesssim 7$ and for $m_0/m_2 = -1.0$. One can see that λ_1 is significantly different from λ_2 , and that λ_2 and λ_3 are degenerate, and similarly, λ_4 and λ_5 are degenerate. As mentioned in the case of two dimensions, this even degeneracy is a consequence of the two symmetries,^{15,16)} the time-reversal symmetry of the Hamiltonian and the supersymmetric structure of the operator A . For the region $W/m_2 \gtrsim 7$ in Fig. 3(a), the diffusive metallic phase appears. In this region, one can see that the above double degeneracy in the spectrum of $A_\Omega^{(\Lambda)}$ is lifted due to the vanishing of the spectral or mobility gap in the metallic phase.

The inset of Fig. 3(a) shows system-size dependences of λ_1 and λ_2 for fixed parameters $m_0/m_2 = -1.0$ and $W/m_2 = 1.0$. As the system size increases, λ_1 and λ_2 converge to 1 and about 0.7, respectively. Thus in the infinite-volume limit, we can clearly conclude that the \mathbb{Z}_2 index ν is unity. One can perform a similar analysis and extract the eigenvalues of A in the infinite-volume limit for other values of the parameters.

As seen in Fig. 3(b), the double degeneracy of $\lambda \simeq 1$ appears in the region of WTI where the corresponding parameter satisfies $m_0/m_2 \lesssim -2$. Clearly, one can see that λ_3 is separated from $\lambda_1 \simeq \lambda_2 \simeq 1$, and hence the \mathbb{Z}_2 index ν is equal to zero. Thus, if the first and the second eigenvalues, λ_1 and λ_2 , are degenerate, information

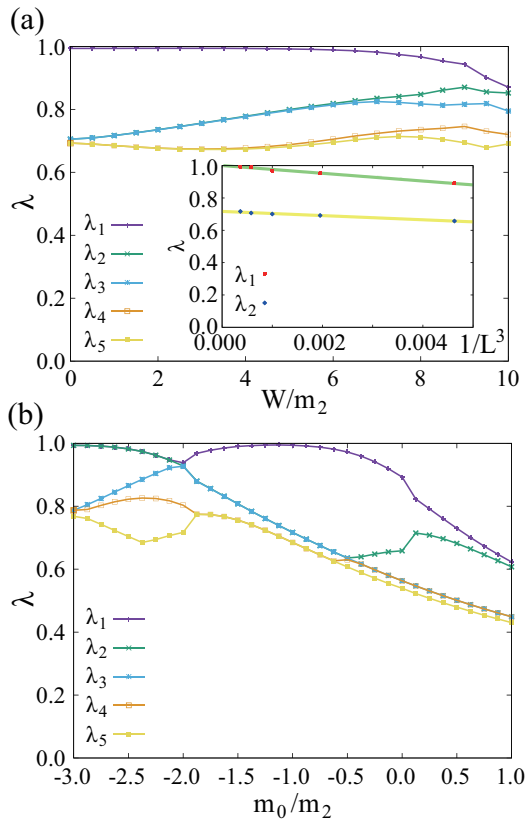


Fig. 3. (Color online). (a) W/m_2 and (b) m_0/m_2 dependences of the eigenvalues λ_i , $i = 1, 2, \dots, 5$, of the operator $A_\Omega^{(\Lambda)}$ for the system size $L^3 = 2744$. (a) and (b) correspond to cross-sections of Fig. 2 for $m_0/m_2 = -1.0$ and $W/m_2 = 1.0$, respectively. The inset in (a) shows λ_1 and λ_2 as a function of the inverse volume of the system ($1/L^3$) for fixed parameters, $m_0/m_2 = -1.0$ and $W/m_2 = 1.0$. The green (yellow) line is a fit to the numerical data of λ_1 (λ_2).

about the third eigenvalue λ_3 is useful to determine the \mathbb{Z}_2 index.

Summary: We have presented our new method for numerically calculating the \mathbb{Z}_2 indices of topological insulators with strong disorder. Our method has the following two advantages: (i) There is no need to take an average of the \mathbb{Z}_2 index over random variables in a model. (ii) The \mathbb{Z}_2 index is determined by the discrete spectrum of a certain compact operator with a supersymmetric structure. These properties make it possible to numerically determine the \mathbb{Z}_2 index highly efficiently. In order to check the effectiveness of our method, we have demonstrated that all of the numerical values of the \mathbb{Z}_2 indices completely coincide with the predictions in previous studies using a reliable transfer-matrix method^{18,19,22}) for the two-dimensional Bernevig-Hughes-Zhang and the three-dimensional Wilson-Dirac models. Thus, the strong topological insulator phases can be characterized by the \mathbb{Z}_2 index in the index formulae,^{15,16}) and can be clearly distinguished from other phases. We believe that the good agreement between the two different approaches is one of the steps toward the understanding of the nature of \mathbb{Z}_2 topological insulators although we cannot definitely compare our method with other approaches mentioned at

the beginning of the present paper. Finally, we remark that the generalization of our method to models in other symmetry classes in arbitrary dimensions is straightforward.

Acknowledgements

The authors acknowledge helpful discussions with Ken-Ichiro Imura, Takahiro Misawa, Tomi Ohtsuki and Synge Todo. This work was supported by JSPS KAKENHI Grant Nos. JP15K17719, JP16H00985, JP17K14352.

- 1) C. L. Kane and E. J. Mele, *\mathbb{Z}_2 Topological Order and the Quantum Spin Hall Effect*, Phys. Rev. Lett. **95**, 146802 (2005).
- 2) L. Fu and C. L. Kane, *Topological insulators with inversion symmetry*, Phys. Rev. B **76**, 045302 (2007).
- 3) Q. Niu, D. J. Thouless, and Y.-S. Wu, *Quantized Hall conductance as a topological invariant*, Phys. Rev. B **31**, 3372 (1985).
- 4) A. P. Schnyder, S. Ryu, A. Furusaki, and A. W. W. Ludwig, *Classification of topological insulators and superconductors in three spatial dimensions*, Phys. Rev. B **78**, 195125 (2008).
- 5) A. Kitaev, *Periodic table for topological insulators and superconductors*, AIP Conference Proceedings **1134**, 22 (2009).
- 6) S. Ryu, A. P. Schnyder, A. Furusaki, and A. W. W. Ludwig, *Topological insulators and superconductors: tenfold way and dimensional hierarchy*, New J. Phys. **12**, 065010 (2010).
- 7) A. M. Essin and J. E. Moore, *Topological insulators beyond the Brillouin zone via Chern parity*, Phys. Rev. B **76**, 165307 (2007).
- 8) H.-M. Guo, *Topological invariant in three-dimensional band insulators with disorder*, Phys. Rev. B **82**, 115122 (2010).
- 9) B. Leung and E. Prodan, *Effect of strong disorder in a three-dimensional topological insulator: Phase diagram and maps of the \mathbb{Z}_2 invariant*, Phys. Rev. B **85**, 205136 (2012).
- 10) I. C. Fulga, F. Hassler, and A. R. Akhmerov, *Scattering theory of topological insulators and superconductors*, Phys. Rev. B **85**, 165409 (2012).
- 11) B. Sbierski and P. W. Brouwer, *\mathbb{Z}_2 phase diagram of three-dimensional disordered topological insulators via a scattering matrix approach*, Phys. Rev. B **89**, 155311 (2014).
- 12) T. A. Loring and M. B. Hastings, *Disordered topological insulators via C^* -algebras*, EPL (Europhysics Lett.) **92**, 67004 (2010).
- 13) T. A. Loring, *K-theory and pseudospectra for topological insulators*, Ann. Phys. **356**, 383 (2015).
- 14) T. A. Loring and H. Schulz-Baldes, *Finite volume calculation of K-theory invariants*, Preprint arXiv:1701.07455 (2017).
- 15) H. Katsura and T. Koma, *The \mathbb{Z}_2 index of disordered topological insulators with time reversal symmetry*, J. Math. Phys. **57**, 021903 (2016).
- 16) H. Katsura and T. Koma, *The Noncommutative Index Theorem and the Periodic Table for Disordered Topological Insulators and Superconductors*, Preprint arXiv:1611.01928 (2016).
- 17) B. A. Bernevig, T. L. Hughes, and S.-C. Zhang, *Quantum Spin Hall Effect and Topological Phase Transition in HgTe Quantum Wells*, Science **314**, 1757 (2006).
- 18) A. Yamakage, K. Nomura, K.-I. Imura, and Y. Kuramoto, *\mathbb{Z}_2 Topological Anderson Insulator*, J. Phys.: Conf. Ser. **400**, 042070 (2012).
- 19) A. Yamakage, K. Nomura, K.-I. Imura, and Y. Kuramoto, *Criticality of the metal-topological insulator transition driven by disorder*, Phys. Rev. B **87**, 205141 (2013).
- 20) K. G. Wilson, *Confinement of quarks*, Phys. Rev. D **10**, 2445 (1974).
- 21) X.-L. Qi, T. L. Hughes, and S.-C. Zhang, *Topological field theory of time-reversal invariant insulators*, Phys. Rev. B

- 78, 195424 (2008).
- 22) K. Kobayashi, T. Ohtsuki, and K.-I. Imura, *Disordered Weak and Strong Topological Insulators*, Phys. Rev. Lett. **110**, 236803 (2013).
- 23) We note that a tight-binding model on an arbitrary lattice in d dimension can be mapped onto the model on \mathbb{Z}^d with suitably chosen hopping integrals.
- 24) J. Avron, R. Seiler, and B. Simon, *The Index of a Pair of Projections*, J. Func. Anal. **120**, 220 (1994).
- 25) Here, $A^{(\Lambda)}$ is expressed in terms of P_F and $\tilde{D}_a(\mathbf{x}) := \mathcal{D}_a(\mathbf{x}) \otimes \mathbb{1}_4$ as $A^{(\Lambda)} = P_F - \tilde{D}_a^* P_F \tilde{D}_a$, where $\mathbb{1}_4$ is the 4-dimensional identity matrix and \mathcal{D}_a should be thought of as a matrix of dimension $|\Lambda|$.
- 26) In this case, the operator $A^{(\Lambda)}$ is written as $A^{(\Lambda)} = \tilde{P}_F - \tilde{D}_a \tilde{P}_F \tilde{D}_a$, where $\tilde{P}_F := P_F \otimes \mathbb{1}_2$, $\tilde{D}_a(\mathbf{x}) := \sum_{i=1}^3 D_a^i(\mathbf{x}) \otimes \mathbb{1}_4 \otimes \sigma_i$, and $D_a^i(\mathbf{x}) := (x_i - a_i)/|\mathbf{x} - \mathbf{a}|$. Here, $\mathbb{1}_2$ and $\mathbb{1}_4$ are the 2- and 4-dimensional identity matrices, respectively. Each operator D_a^i should be thought of as a matrix of dimension $|\Lambda|$.
- 27) L. Fu, C. L. Kane, and E. J. Mele, *Topological Insulators in Three Dimensions*, Phys. Rev. Lett. **98**, 106803 (2007).